Protocols

In vitro model of the outer blood–retina barrier

H. Steuer, A. Jaworski, D. Stoll, B. Schlosshauer*

Natural and Medical Sciences Institute (NMI) at the University Tübingen, Markwiesenstr. 55, D-72770 Reutlingen, Germany

Abstract

The outer blood–retina barrier (BRB) is formed by the retinal pigment epithelium (rpe) and functions similarly to the blood–brain barrier (BBB). In contrast to the BBB, which is composed of a myriad of capillaries, the rpe can in principle be prepared as an intact planar tissue sheet without disruption of its barrier and carrier functions. Both a rapid and gentle procedure to isolate porcine rpe and a method to implement the harvested rpe in drug penetration testing are presented. Enucleated eyes were flat-mounted and the RPE/choroid tissue sheets with or without the retina were isolated. Fluorescence microscopy based on double-labeling with propidium iodide/calcein and scanning electron microscopy revealed well-preserved cell and tissue architecture. For drug evaluation, specimens were immobilized as the interface between test compartments in a dual-chamber device. Ten different test agents were added to one chamber at defined concentrations. After an incubation time of 30 min at 37 °C permeated drug levels in both compartments were quantified by HPLC-tandem mass spectrometry or HPLC with fluorescence detection. Sodium fluorescein used as a barrier marker indicated that the rpe model had excellent seal integrity. The use of a representative subset of pharmaceuticals with known BBB permeability characteristics demonstrated that the rpe model had a large permeability dynamic range (factor >350). These findings showed that the model represents a valuable tool for the investigation of the blood barrier penetration of test compounds.

1. Type of research

- Blood–brain and blood–retina barrier [34,37,41,44]
- In vitro models [17,27,33]
- Pharmacology, pharmacokinetics, toxicology, cell biology [11,22,36]

2. Time required

The time required to run the total protocol including transport of the eyes from the abattoir, biological experiments and analysis is 4 h to 3 days, depending on the analytical method used and the number of assay repetitions. After the eyes have arrived at the laboratory, the processing can be subdivided into three distinct periods:

- Rpe dissection and initiation of short-term culturing, which requires about 10 min for each specimen.
- Test agent application and subsequent sample collection takes about 45 min.
- Analysis: 20 min for calcein/propidium iodide labeling plus 1 h fluorescence microscopy, 1.5 days for scanning electron microscopy. HPLC-tandem MS method development takes 1–2 days for each component. Analysis times for each sample are dependent on the respective method and usually ranges between 10 and 15 min per sample for HPLC-tandem mass spectrometry or HPLC with fluorescence detection. Data analysis and documentation takes one additional day.

* Corresponding author. Tel.: +49-7121-51530-20; fax: +49-7121-51530-16.

E-mail address: schlosshauer@nmi.de (B. Schlosshauer).

3. Materials

3.1. Special equipment

3.1.1. Preparation

- Dissecting base: interior polystyrene, exterior aluminum foil (homemade), paraffin-filled dissecting dish, dissecting needles, preparation tools, sterile compresses
- 24-well tissue culture plate (#3527, Corning)

3.1.2. Microscopy

- Image acquisition system: microscope (Axiovert 35M, Zeiss, Germany), microscope camera (Hamamatsu, Nippon), Software (Leica QWin)
- Scanning electron microscope (S100, Cambridge Instruments)

3.1.3. Drug penetration assay

- Perfusion system composed of a polycarbonate chamber (4 × 4 × 4 cm) with two sub-compartments (each 0.5 ml in volume) and four in-/outlets with fittings for clinical syringes; a reverse hinge and metal clamp in front allow for convenient sealing (Minucells and Minutissue, Bad Abbach, Germany).
- Cell culture incubator (Heraeus, Hanau, Germany)
- Sterile 1 ml one-way syringes (Braun, Melsungen, Germany)
- Centrifuge tubes (50 ml, #610261, Greiner, Nürtingen, Germany)

3.1.4. Quantitative analysis of test agents

- Model 1100 HPLC system (Agilent) comprising of degasser, binary pump, autosampler, thermostatic column compartment connected either to a triple–quadrupole-mass spectrometer Quattro Micro (Micromass) equipped with an electrospray ion source or to a fluorescence detector L 7400 (Merck-Hitachi).
- Set of stationary phases for chromatographic separation of compounds: (1) Aqua 5 μ C18 125A, 50 × 2 mm (Phenomenex); (2) Kromasil 3.5 μ C18, 50 × 2 mm (Phenomenex); (3) Kromasil 3.5 μ C8, 50 × 2 mm (Phenomenex); (4) Luna 3.5 μ C18 (2) 30 × 2 mm (Phenomenex); (5) Chromolith SpeedROD C18e 50 × 4.6 mm (Merck); (6) Grom-Sil Vinyl-1 Fe 3 μ 60 × 2 mm (Grom).
- HPLC amber-glass vials (12 × 32 mm), screw neck (#854983, Sigma), screw caps PTFE/silicone (#854984, Sigma).
- Ultrapure water (>18.3 MΩ cm^{-1}, from in-house Membra Pure equipment), Acetonitrile gradient grade (SDS), formic acid, puriss p.a. (Sigma-Aldrich), ammonia solution, p.a. (Roth); ammonium hydroxide 1 M in water (Riedel de Haen).

3.2. Chemicals and reagents

- Calcein AM (#C-3100, Molecular Probes), propidium iodide (#P-4170, Sigma-Aldrich), dimethyl sulfoxide (DMSO) (#D-5879, Sigma-Aldrich), Hank's balanced salt solution (HBSS) (#H22-008, PAA, Germany), isopropanol, glutardialdehyde, paraformaldehyde (Merck), physiological NaCl solution, 70% ethanol, acetone, phosphate-buffered saline (PBS), bovine serum albumin (BSA), Triton X-100 (#X-100, Sigma), mowiol.
- Sodium fluorescein (#F-6377, Sigma), caffeine (#27600, Fluka), memantine hydrochloride (#M-9292, Sigma), L-nicotine (#36733, Riedel de Haen), clonidine hydrochloride (#C-7897, Sigma), cimetidine (#C4522, Sigma), rhodamine 123 (#R-8004, Sigma), verapamil hydrochloride (#V-4629, Sigma), gabapentin (graciously provided by Schering), probenecid and atenolol (provided by Bayer).

4. Detailed procedure

4.1. Preparation of retinal pigment epithelium

Immediately after sacrificing the pig in the abattoir, enucleate both eyeballs and store them for transport in ice-cold 0.9% NaCl.

- Remove muscle and connective tissue from the bulbus surface.
- Rinse eyeball 5 s in 70% ethanol.
- Cut the eye parallel to the limbus 3–5 mm behind the iris–lens–diaphragm and remove the anterior eye segment [12].
- Remove the loosely associated vitreous.
- Immobilize the eye cup in a dissecting dish and cover the specimen with ice-cold HBSS, pH 7.4.
- Separate the sclera from the choroid for a few millimeters all around the specimen, leaving the retina/rpe/choroid unaffected (for simplicity, rpe/choroid tissue sheets both with and without retina are termed "*rpe tissue sheet*".)
- With the rpe tissue still attached to the sclera, cut the rpe into small pieces as needed, e.g. for immunohistochemistry, vital staining or mounting in the perfusion chamber.
- Remove the rpe tissue from the sclera.
- Mount each rpe tissue fragment carefully, e.g. onto adhesive nitrocellulose filter sheets, or proceed without using any mechanical support.
- Collect rpe tissue segments in a 24-well plate in HBSS, keeping the HBSS cold.
- For viability and integrity studies, the retina must be removed to allow direct optical monitoring of rpe cell surfaces.

4.2. Cytochemistry/microscopy

4.2.1. Calcein and propidium iodide staining

- To stain viable and dead cells, prepare stock solutions as follows: calcein AM (1 μg/μl DMSO, storage at 4 °C) and propidium iodide (333 μg/ml H$_2$O, storage at − 20 °C).
- Dilute stock solutions 1:200 (calcein AM) and 1:100 (propidium iodide) in HBSS (staining solution).
- Incubate rpe tissue without retina in a multi-well plate filled with staining solution (20 min at 37 °C).
- Wash rpe tissue twice with HBSS and inspect microscopically for cell viability (Zeiss Axiovert 35 M, 10 × and 40 × Neofluar, excitation/observation calcein 480/>505 nm, propidium iodide 546/>570 nm). Calcein AM diffuses freely into viable cells and is then cleaved by esterases; the resulting fluorescent calcein is trapped intracellularly if cell membranes are intact. Dead cells are marked by propidium iodide, which intercalates with DNA and can penetrate only permeabilized membranes. Viable cells display green fluorescence, whereas dead cells exhibit red cell nuclei.

4.2.2. Scanning electron microscopy

- Fix specimens consecutively in 4% paraformaldehyde (in PBS, 30 min, 22 °C) and 2% glutardialdehyde/4% paraformaldehyde (in PBS, 16 h, 22 °C).
- Dehydrate specimens in a series of increasing concentrations of isopropanol/H$_2$O.
- Critical point dry specimens as described in Ref. [20]
- Sputter specimens with gold.
- Employ a scanning electron microscope to visualize rpe explant surface structures.

4.3. Permeability studies of test compounds

- Prepare test compound stock solutions as follows: sodium fluorescein (30 mM in H$_2$O), caffeine (100 mM in H$_2$O), memantine hydrochloride (1 mM in H$_2$O), nicotine (1 M in ethanol), clonidine hydrochloride (6 mg/ml in H$_2$O), cimetidine (6 mg/ml in H$_2$O), rhodamine 123 (0.4 mg/ml H$_2$O), verapamil hydrochloride (1.5 mM in H$_2$O), gabapentin (1.7 mM in H$_2$O), probenecid (5 μg/μl in DMSO) and atenolol (5 μg/μl in ethanol). Dilute test agent stock solutions with HBSS to yield a concentration that is convenient for mass spectrometric analysis. Typically, concentrations of 10–100 μM in the donor chamber result in test agent concentrations in the acceptor chamber that are still above the detection limit.
- Pre-incubate preparations, chambers, and syringes at 37 °C.
- Place the rpe tissue sheet into the test apparatus with the tissue at the interface of the perfusion chambers. Close the lid to hold the rpe tissue in place and seal both compartments. The fastened metal clamp provides sufficient pressure to prevent leakage.
- Fill the donor chamber (chamber on the choroid side of the rpe tissue sheet) with the test agent solution.
- Fill the acceptor chamber with HBSS. Take care neither to import air bubbles nor to overfill the chambers, as the exact volume is needed for the calculation of the permeability coefficient.
- Incubate for 30 min at 37 °C in a humidified atmosphere.
- After incubation, separately aspirate the solutions completely from the donor and acceptor chamber. Transfer collected solutions into HPLC amber-glass vials.
- HPLC-tandem-mass spectrometric analysis. Tune instrument for each component to obtain limits of quantification in the picomolar to low nanomolar range. First optimize instrument settings of the ion source and Q1 to generate the protonated pseudomolecular ion $[M+H]^+$ of the compound of interest. Introduce the compound into the MS by a syringe pump (100 pg/ml in ACN/H$_2$O 1:1 v/v, at a flow rate of 5 μl/min). Change instrument settings (cone volts, capillary volts, extraction cone, RF-settings) and watch the resulting changes of the ion signal closely. Use parameters that indicate highest ion-count for the respective compound. Perform MS/MS fragmentation by increasing the pressure of argon in the collision cell up to 2–3.5 mbar and by changing collision energy until a fragment spectrum is detected in Q2. Determine the most suitable collision energy by observing the response of a selected fragment ion after systematic changes in collision energy and argon pressure.
  For optimization of HPLC parameters, carry out HPLC-MS/MS analysis of each compound in the multiple reaction monitoring mode (MRM) using the optimized instrument parameters of the mass spectrometer for Q1 and Q2. According to hydrophobicity and pKs of compound of interest select suitable stationary phase and eluents (see below). Perform HPLC-MRM analyses to discover sample carry-over, LOD, LOQ, linear detection range and reproducibility of HPLC-MS/MS method.
- Calculate the permeability coefficients with the following formula,

$$P_e = dx/dt \times (C \times A)^{-1}$$

where P_e is the permeability coefficient (cm/s), dx/dt is the rate of translocation (pmol/s), C is the initial concentration of the drug in the donor chamber (pmol/cm^3) and A is the area of penetration (cm^2) [26].

5. Results

5.1. Methodological aspects

In initial experiments we determined which species is best suited for the preparation of BRB, based on logistical,

experimental and functional aspects. Chicks, pigs, sheep, and cows were considered as potential donors. The availability of enucleated eyes was ascertained, based on transport distances and the schedules of local abattoirs, resulting in the preference: pig>cow>sheep>chick. Cow specimens provide the largest tissue mass. Pig eyes resemble the human eye to the highest degree, whereas chicks are evolutionarily most distant from humans and are fairly small [2,25,45]. Cow and sheep eyes have circumscribed tissue areas devoid of pigmentation and proximate to a fibrous layer (tapetum lucidum) that is absent in humans and pigs [28]. Since cow and sheep eyes contain these clearly defined pigmented and nonpigmented areas, comparative investigations on the impact of melanin become feasible. However, the restricted diffusion properties of the tapetum lucidum should be taken into account for penetration studies. Another aspect to consider is whether the retina can be removed or must be kept in association with the rpe. In principle, it was found that all analyzed species allow for both configurations with different degrees of restrictions. Pig retina and rpe can be detached with the least effort, i.e. without enzyme treatment and chelators. Taking all these aspects into account, we focused on the porcine eye for most studies.

5.2. Tissue preparation and perfusion chamber

The core elements of the porcine eye are retina, rpe, choroid and sclera (Fig. 1A,B). Fenestrated blood vessels are found in the sponge-like choroid. Blood-borne components diffuse out of the choroid and reach the outer retina via the rpe, which represents the outer blood retina–barrier with features comparable to the endothelial blood–brain barrier (BBB) [7,37]. The rpe is composed of a single layer of cells closely associated via tight junctions. In order to preserve the barrier function, it was essential to retain the close apposition between the rpe and the choroid. The sclera was removed (see scheme Fig. 1B), whereas for all subsequent studies the retina was kept in place. The dissection began with removal of muscles and connective tissue and the anterior eye cap (Fig. 1C). After removing the vitreous, the posterior bulbus was immobilized on the preparation dish. During the following step, specimens (retinal pigment epithelium-choroid with or without retina; collectively called "rpe tissue sheet") were prepared as a single tissue sheet.

The first series of investigations were performed to establish how long tissue integrity was retained after extended storage. Enucleation was performed within 5 min after killing the animal. Transport at 4 °C to the laboratory took less than 45 min. Thereafter, intact eyeballs were stored at either 37 °C or 4 °C for various time intervals. To determine cell viability, 12–20 rpe tissue sheets without retina were dissected after the different storage times and double-labeled with calcein and the nuclear stain propidium iodide. Fluorescence microscopy

revealed that at 4 °C, viability of rpe cells remained unchanged for at least 2 h and declined thereafter. In contrast, viability dropped to about 50% after only 1 h at 37 °C, with a further decline to less than 10% after 2 h. Complete cell deterioration was observed after 4 h at 37 °C, but only after 24 h at 4 °C (Fig. 1E). Specimens kept at room temperature resembled those at 4 °C (data not shown). It is noteworthy that tissue integrity varied considerably even at time point $t = 0$, which is reflected by the fact that, e.g. at 4 °C, along with the 15 fully viable specimens, three rpe tissue sheets displayed partial deterioration. This variability may be due to inappropriate handling at the slaughterhouse or physiological differences between individual animals. These results emphasize the importance of using controls for individual specimens during functional assays (see below). No significant differences between unbuffered 0.9% NaCl solution and glucose-containing buffered salt solutions were observed (data not shown). Therefore, anoxia rather than hypoglycemia or acidification appears to have been the primary adverse effect of long-term storage at elevated temperatures.

For subsequent pharmacological evaluations, rpe tissue sheets were immobilized in a convenient two-chamber polycarbonate device (Fig. 1F,G). A rpe tissue sheet was used as the interface between the donor and acceptor chambers. Due to elastic rings at the chamber interface, both compartments could be hermetically sealed once the lid containing the donor chamber had been closed and latched with a single metal clamp (Fig. 1G). Solutions could be easily added to and removed from the donor and acceptor chambers via four openings without affecting rpe tissue sheets (Fig. 1F). The open diameter of the tissue sheet was 3 mm and the interface area was about 7 mm^2. Thus, one porcine eye provided two to four individual rpe tissue sheets.

5.3. Tissue integrity

Tissue integrity was tested after preparation by means of fluorescence and scanning electron microscopy. The most delicate structures of the rpe are the microvilli, which interdigitate in situ with photoreceptors of the neural retina [21]. As revealed in Fig. 2A and B, microvilli are well-retained in both porcine and bovine specimens. Since this type of analysis could not qualify cell viability and cell–cell contact sites among rpe cells, flat-mounted rpe tissue sheets without retina were co-incubated with: (a) calcein, which marks only viable cells, and (b) propidium iodide, which exclusively labels dead cells by intercalating into DNA. Fig. 2C displays excellent preservation of cell contact sites, as judged from the continuous hexagonal pattern outlining the circumferences of rpe cells, and additionally reflects the optimal cell viability achieved. No labeling with propidium iodide was observed (not shown). To demonstrate the functionality of the DNA
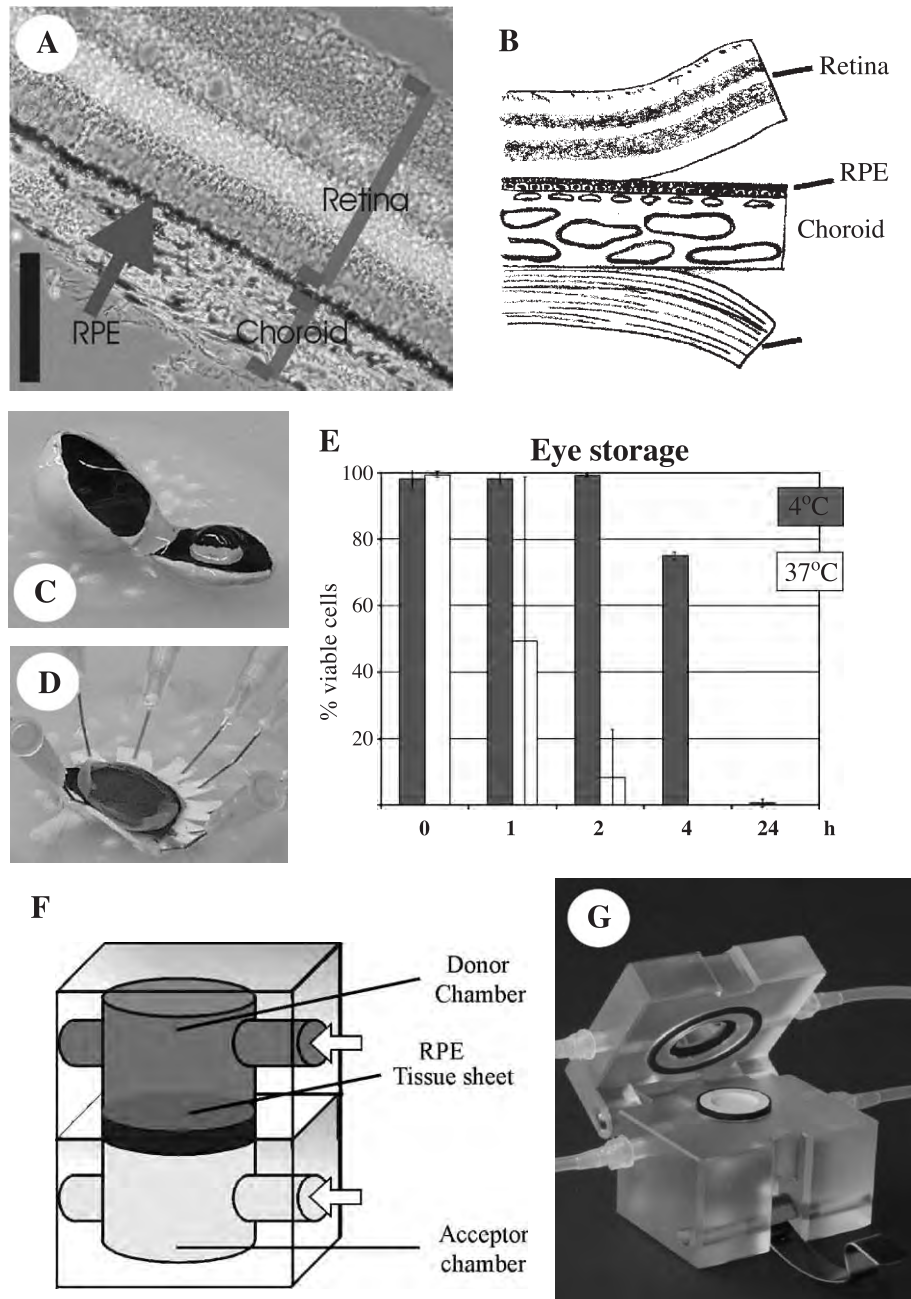
Fig. 1. Tissue preparation and perfusion chamber. (A) Phase contrast-fluorescence double image of a cross-section of the porcine eye. Vitreous and sclera had been previously removed. Cell nuclei appear light due to fluorescent DAPI labeling. The retinal pigment epithelium (RPE) separates the neural retina from the choroid, which contains blood vessels. (B) Schematic representation of different eye layers. Retina and sclera can be removed from the rpe/choroid tissue layers. Blood vessels of the choroid are indicated by circular structures. (C) Dissection of the porcine eye. The anterior portion of the bulbus including the lens is eliminated first; (D) thereafter, the retina/rpe tissue sheet is separated from the posterior bulbus tissue. (E) Eye storage. Rpe cell survival during storage of intact eyeballs is critically dependent on the temperature. The percentage of surviving rpe cells was determined via fluorescent labeling with calcein after time periods varying between 0 and 24 h at both 4 and 37 °C. (F) Schematic drawing of the perfusion system, which is composed of a donor and an acceptor chamber. The rpe tissue sheet is placed between the two compartments. Arrows indicate two inlets for application of buffer solutions. Test agents are added to the donor chamber, permeated agents are collected from the acceptor chamber. (G) Perfusion system, with the donor chamber located in the lid and the acceptor chamber in the base. Scale bar: (A) 100 μm.

labeling technique, in control experiments rpe tissue sheets were paraformaldehyde fixed and incubated with propidium iodide; Fig. 2D shows the marked cell nuclei of a fixed, flat-mounted rpe tissue sheet.

5.4. Pharmacological evaluation

Though the above experiments suggest that the established dissection procedure in principle provides valuable
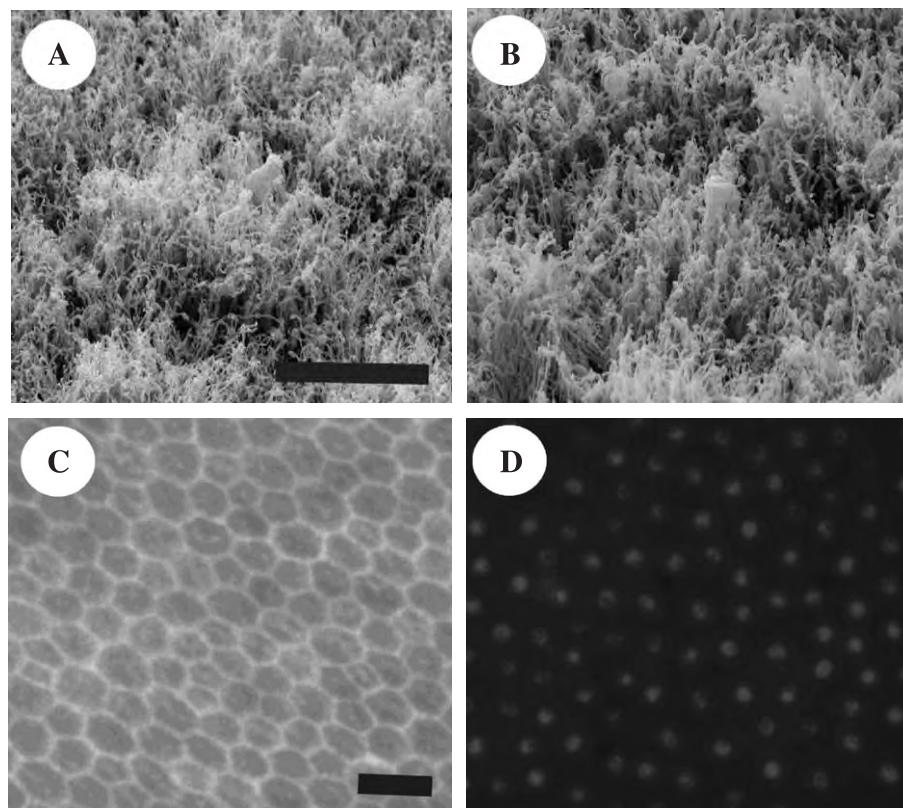
Fig. 2. Isolated retinal pigment epithelium. (A, B) Scanning electron micrograph of porcine (A) and bovine (B) retinal pigment epithelium. The gentle dissection procedure preserves the microvilli structures of rpe cells. (C, D) Fluorescence micrographs of flat-mounted porcine rpe tissue sheets. (C) Calcein AM/propidium iodide double-labeling reveals cell viability and intact cell–cell contact sites, as judged from the continuous hexagonal cell morphologies. Note that no nuclear staining that would be indicative of dead cells is evident (D). In contrast, the negative control, an experimentally permeabilized specimen, displays no calcein AM labeling but exhibits staining of rpe cell nuclear DNA. Bars 10 μm (A for A and B), 30 μm (C for C and D).

specimens, it was neither known if barrier function had been preserved nor if each individual rpe tissue sheet was indeed intact. In humans, vitreous fluorophotometry with fluorescein derivatives is widely employed to monitor the status of the blood–retina barrier [5]. Similarly, we applied sodium fluorescein (Na-fl) to rpe tissue sheets (with attached retina) that had been sealed into perfusion chambers as outlined above. A high concentration (300 μM) of Na-fl was added to the donor chamber at 37 °C, with the basal (i.e. choroidal) side of the rpe facing the donor chamber. Samples were collected from donor and acceptor chambers 30 min later and analyzed by HPLC using a fluorescent detector. Histological analysis after calcein/propidium iodide double-labeling revealed partially disrupted cell–cell contact sites in rpe tissue sheets with a permeability coefficient (P_e) significantly greater than 5×10^{-7} cm/s. Since it was not possible to judge the quality of specimens simply based on the dissection procedure, individual rpe tissue sheets were qualified using Na-fl permeation in all subsequent experiments. Specimens with $P_e > 5 \times 10^{-7}$ cm/s were excluded from further analysis. Whereas the observed P_e of our rpe tissue sheets in vitro is within the observed in vivo range, most other in vitro blood–brain barrier models were reported to have a higher P_e and thus

appear to provide reduced barrier integrity [13,15,16,24,29] (Fig. 3A).

To determine the dynamic range and selectivity of rpe tissue penetration, various test compounds with known in vivo BBB permeability characteristics were employed as described above and quantified by liquid chromatography/tandem mass spectrometry, which has been shown to be a fast and highly sensitive method to determine pharmacological agents from blood–brain barrier models [4,38]. The 10 different compounds (memantine, nicotine, verapamil, clonidine, gabapentin, probenecid, cimitidine, rhodamine 123, Na-fl, and atenolol) [1] displayed P_e over a dynamic range of more than 350 units, with the highest value ($P_e = 3.17 \times 10^{-5}$ cm/s) for memantine, an NMDA receptor antagonist that exhibits pronounced BBB penetration and is used to treat Alzheimer's disease [30,35], and the lowest ($P_e = 9.06 \times 10^{-8}$ cm/s) for atenolol (Fig. 3B). Atenolol does not cross the BBB in vivo and is used as a β-receptor antagonist to treat coronary disease [42]. In summary, the rpe tissue sheet allows classification of permeation into three major categories: poor permeation of about 10^{-7} cm/s, moderate permeation of about 10^{-6} cm/s, and pronounced permeation, with a P_e of about 10^{-5} cm/s. Thus, the model represents an in vitro technique implementing the

A   **System comparison:**

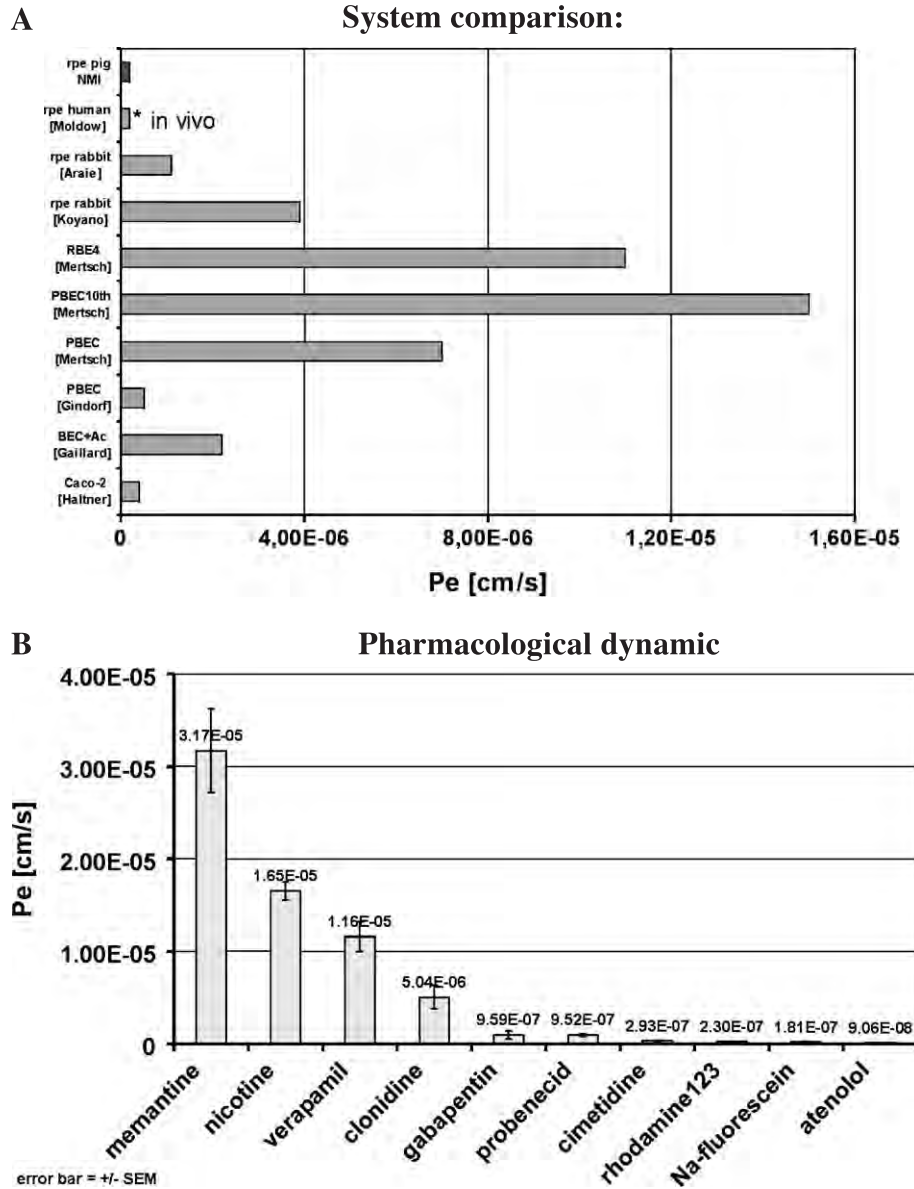**B**   **Pharmacological dynamic**

Fig. 3. Pharmacological evaluation. (A) Na-fluorescein as an integrity marker was applied to porcine rpe tissue sheets used as the interface in the perfusion system. The permeability coefficient P_e, determined by HPLC/fluorometry, was compared with P_e values for Na-fluorescein reported for other in vitro systems. The NMI rpe system displays very high integrity. RBE4, transfected rat brain endothelial cell line; PBEC, porcine brain capillary endothelial cells; 10th, tenth passage; BEC + Ac, brain capillary endothelial cell/astrocyte coculture; Caco-2, human adenocarcinoma cell line; P_e, permeability coefficient; authors of cited articles in angular brackets [3,13,15,16,23,29,32]. (B) Determination of test agent P_e. Test agent concentrations in both chamber compartments were quantified 30 min after pharmaceuticals had been added to the donor chamber of perfusion systems containing rpe tissue sheets. The acute rpe model displays a large permeability dynamic range (factor >350).

outer blood–retina barrier, and offers researchers a valuable tool for predicting in vivo drug BBB permeability.

6. Discussion

The major objective of our studies was to establish an in vitro model of the outer blood–retina barrier with relevance for human pharmacological drug profiling studies, which are valuable in ophthalmology [12,14,31]. Additionally, such a system could potentially be employed as a more

general blood–brain barrier (BBB) model [37]. Although there are several in vitro models mimicking the BBB, they all involve destruction of the BBB, as this is technically a prerequisite for isolation of the capillaries or capillary-forming cells [8,10,14,31,43]. Due to its morphology, rpe is basically the only blood–neuronal barrier tissue that can be isolated as an intact planar tissue sheet. The rpe is positioned between the retina, which is an integral part of the central nervous system, and the choroid, which has blood vessels devoid of BBB characteristics [28]. Both the analysis of our preparation and test procedure and the

pharmacological evaluation of the resulting tissue model revealed that the system is valid. Nevertheless, some difficulties might arise; solutions for these problems are presented below.

6.1. Troubleshooting

6.1.1. Tissue integrity

The quality of the porcine eyes was initially quite erratic; thus, we developed the following guidelines for tissue handling: (a) eyes must be removed immediately after sacrificing the animal, as a major cause for tissue deterioration appears to be disruption of circulation at body temperature. (b) The tissue must be rapidly cooled since it cannot be immediately re-oxygenated. Dynamic cooling using agitation and electrical cooling might also be used. (c) Occasionally, normal pigmentation of specimens appeared to have been disturbed, as some rpe tissue samples exhibited bleached areas (no albino phenotype was observed). In some cases, functional testing of these specimens revealed poor barrier properties. Therefore, inspection of rpe tissue and elimination of all specimens with affected pigmentation is strongly recommended. (d) Tissue integrity could additionally suffer due to inappropriate pH. For tissue preparation and pharmacological testing, we employed HBSS pH 7.4, which contains glucose and therefore supports basic energy metabolism. Since HBSS pH increases once exposed to low atmospheric CO_2 concentrations, phenol red indicator could be added for visual pH control. Readjustment of the pH should be performed if necessary. However, it should first be determined whether subsequent HPLC-tandem mass spectrometry will be disturbed by addition of phenol red or HEPES (for pH stabilization).

6.1.2. Assay procedure

To determine the permeability coefficient, the exact sample volume must be ascertained, thus requiring total recovery of the test agent from the donor and the acceptor chambers. Be sure to always fill both chambers with defined and reproducible volumes and avoid any air bubbles, inspecting both chambers visually. If air bubbles are present, aspirate and refill the chamber repetitively while tilting it gently back and forth. During this process, avoid damage to the rpe tissue sheet.

The total recovery of test agents may be impeded due to adhesion to material surfaces. Although recovery rates for fluorescein were >96%, some lipophilic pharmaceuticals displayed pronounced adhesion to polymer surfaces such as polycarbonate. Therefore, minimize the surface area of chambers, tubes, pipette tips, etc., contacted by the test agents to a minimum and reduce contact times between samples and material surfaces as much as possible. Avoid autoclaved pipette tips, as we found them to have highly adhesive characteristics. Bonding with test agents might be also reduced by coating material surfaces with saturating concentrations of blocking buffer containing, e.g. milk powder or polyvinyl pyrrolidone.

6.1.3. Quantification of test compounds by HPLC-tandem mass spectrometry

Analyses of test agents were carried out by HPLC followed by fluorescent detection (fluorescein and rhodamine) or HPLC-MS in the MRM-mode (other compounds, Table 1). In all cases, low quantification limits could be obtained due to the great selectivity and sensitivity of this operation mode for small compounds. As an example the optimization procedure for the HPLC-MS/MS analysis of nicotine is discussed. The pseudomolecular ion $[M+H]^+$ of nicotine at m/z 163.1 Da was chosen as precursor ion for MS/MS-fragmentation. Employing the best fragmentation conditions the mass spectrum of the daughter ions of m/z 163.1 Da was recorded (Fig. 4). The fragment ion at m/z 130.0 Da had the highest intensity and was thus chosen as daughter ion for MRM experiments with an ion transition m/z 163.1 Da $\rightarrow$ 130.0 Da (indicated by the arrow in Fig. 4B).

Table 1
Analytical parameters for different compounds

Compound	Detection method	Eluents	Column no.	Ex/Em of FLD (nm)	Ion Transition (Da)	LOQ	Concentration range of linear detector response
Fluoresceine	FLD	1	5	495/518	–	190 pM	190 pM–600 nM
Atenolol	ESI+	1	3	–	267.1 → 189.7	640 pM	640 pM–400 nM
Clonidine	ESI+	3	6	–	229.9 → 159.8	3.2 nM	3.2 nM–2.0 μM
Diazepame	ESI+	3	4	–	284.9 → 153.9	25.6 pM	25.6 pM–800 nM
Gabapentine	ESI+	3	1	–	171.9 → 137.0	210 pM	210 pM–400 nM
Memantine	ESI+	3	6	–	180.0 → 107.0	256 pM	128 pM–400 nM
Nicotine	ESI+	2	2	–	163.2 → 130.2	640 pM	640 pM–400 nM
Probenecid	ESI+	3	4	–	283.7 → 139.9	640 pM	640 pM–400 nM
Rhodamine	FLD	1	5	522/560	–	2.5 pM	2.5 pM–5 nM

Eluents (1) A: 100 mM NH_4/HCOOH, pH 6.0; B: ACN; (2) A: 100 mM NH_4/HCOOH pH 4.0; B: ACN; (3) H_2O + 0.05% HCOOH, ACN + 0.05% HCOOH. Analytical parameters, LOQ and linear detection ranges for the different compounds used in experiments with the new BBB model. Electrospray mass spectrometry (positive ion mode, ESI+) and fluorescence detection (FLD) were used after HPLC separation of components. For FLD the excitation and emission wavelengths are listed in the table, whereas for tandem mass spectrometry the ion transitions used for MRM detection are given. Linear gradients (5–95% solvent B) were used for separation of compounds. Cimetidine, coffeine and verapamil were analyzed by Bayer Service.
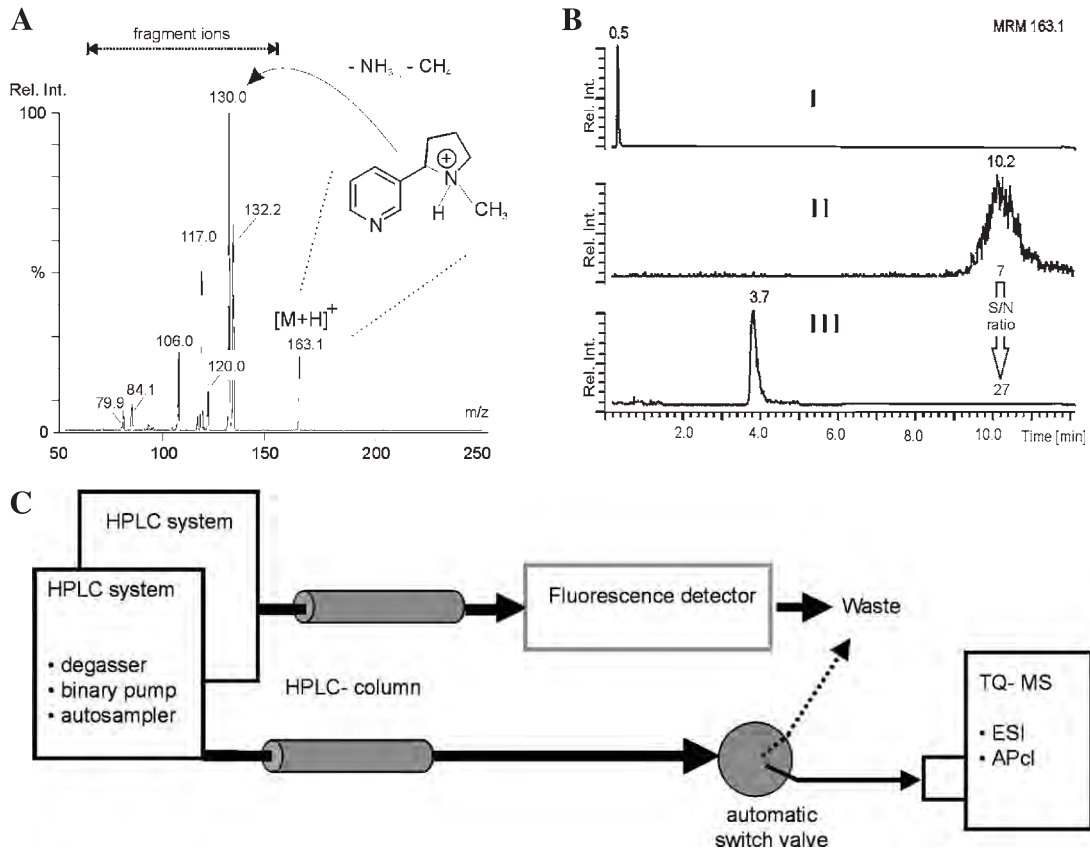
Fig. 4. (A) Mass spectrometry. Fragment ion mass spectrum of nicotine. After fragmentation of the pseudomolecular nicotine parent ion ([M+H]$^+$, 163.1 Da) several fragments were detected showing different ion intensities. The most abundant ion (130.0 Da) was selected as fragment ion for MRM based quantification of nicotine in samples from the blood–brain barrier assay. (MRM ion transition m/z 163.1 Da → 130.0 Da). (B) Optimization of HPLC conditions. Nicotine as a basic substance dissolved in water is completely protonated and therefore, not retained on a C18 RP-HPLC column (column 2, upper trace). When dissolved in HBSS buffer, nicotine was retained on the same C18 RP-HPLC column and eluted as a broad peak (mid-trace). Changing elution conditions from strongly acidic (pH 1–2) to mild acidic (pH 6.0) nicotine was eluted as a sharp, well-defined chromatographic peak (lower trace). The signal to noise ratio increased from 7 to 27 and consequently, with optimized chromatographic conditions lower LOD and the LOQ were observed. (C) Schematic setup. Quantification of fluorophores was performed using the HPLC system directly coupled to the fluorescence detector. Pharmaceutical analytes were quantified using the HPLC system coupled to the electrospray ion source of the triple quadrupole mass spectrometer. An automatic switching between the outlet of the HPLC system and the ion source enabled to divert salt contamination eluting from the HPLC column to waste to prevent contamination of the ion source. This enhanced method reproducibility and system stability significantly.

An enormous enhancement in stability and reproducibility of mass spectrometric quantification for a large number of analyzed samples was observed, when hydrophilic salts and HBSS buffer components were not allowed to enter the ion source of the mass spectrometer. Therefore, an automated divert valve was installed between the outlet of the HPLC system and the MS ion source.

As the retention of test compounds on stationary HPLC phases is very much dependent on the chemical properties of these compounds, a thorough selection of the optimal stationary phase can increase LOD and LOQ significantly. For basic drugs like nicotine dissolved in acidic or neutral buffers the retention to RP-HPLC phases is often not sufficient; e.g. a nicotine standard dissolved in H$_2$O was not retained on the HPLC column (column Nr. 2/Kromasil C18) and eluted within the dead volume of the system when acidic elution buffers were used (Fig. 4B, upper trace). The same nicotine amount dissolved in HBSS-buffer was totally retained on the same stationary phase and eluted as a brought peak when the same acidic elution buffers were used (Fig. 4B, mid-trace). Changing the pH of the elution buffers from very acidic (pH 1–2) to weak acidic conditions using 100 mM ammonia formate buffer (pH 6.0) and pure acetonitrile without additives, nicotine was eluted from the same HPLC column in a sharp, well-defined peak (Fig. 4B, lower trace). By this modification of the elution buffer, the signal to noise ratio changed by a factor of 4, from 7 to 27. This clearly shows that the limit of quantification is not only dependent on optimal tuning of the mass spectrometer but also on the optimization of chromatographic conditions. Therefore, care must be taken to optimize both, mass spectrometric detection parameters and chromatographic conditions for each substance to enable detection of pharmacological agents in the low nanomolar range.

6.2. Alternative and support protocols

Alternatively to our acute preparation of intact rpe-choroid tissue, single cell cultures can be employed. Here, rpe cells are detached mechanically from the choroid and retina, isolated, and the apical side of the cells is then attached to an adhesive gelatin matrix [19]. The gelatin matrix was used to lift off rpe cells. In another approach, trypsinized rpe cells were enriched via percoll density gradient centrifugation [6]. Subsequent culturing of cells was performed on different substrata including fibronectin, laminin or a basal lamina produced by bovine corneal endothelial cells originating from domestic pigs [39]. By seeding the cells onto coated semipermeable membrane filters, transport studies are made possible. However, such cultures are time-consuming and are typically accompanied by various degrees of cell de-differentiation [18].

In order to prevent cell de-differentiation and preserve nearest neighbor relationships of cells, 4 mm eye wall explants including the rpe, choroid and sclera can be prepared [9]. Though the sclera represents a considerable diffusion barrier and contributes to the outer blood–retina barrier formed by the rpe, the eye wall preparation was employed for drug transport assays. In addition to our hinge-type perfusion chamber, the commercially available Ussing chamber could be used. The Ussing chamber has been employed in conjunction with eye wall specimens because it allows for immobilization of a tissue sheet between two chamber compartments [24,40]. For prolonged culture periods, both perfusion and electrical measurements can be performed via different in- and outlets in the chamber. Alternatively, rpe tissue sheets can be placed in a perfusion container holding up to six specimens in a row [12]. Though a permanent culture medium flow is present, guaranteeing tissue survival, the enhanced metabolism of the retina limits the use of such a multiple approach (personal observations). Another limitation of this system is the inability to address both tissue surfaces separately.

7. Conclusion

The current protocol based on a recent approach [12] provides a rapid and gentle means to isolate the porcine outer blood–retina barrier as intact tissue. Due to the considerable similarities between human and porcine tissue morphology and physiology [28], the porcine model promises to be a valuable tool to investigate pharmacological, toxicological and mechanistic aspects during drug administration. The combination of rpe tissue sheets and the convenient dual-compartment perfusion chamber will be a valuable resource in ophthalmology and pharmaceutical drug profiling. Agents with central nervous system (CNS) targets and therapeutic components whose potential CNS side effects must be analyzed in safety pharmacology studies can be tested.

8. Quick procedure

1. Collect, transport, and rapidly process enucleated porcine eyes at 4 °C.
2. Dissect the rpe tissue sheet by removing the anterior bulbus and sclera at 4 °C.
3. Prepare pharmacological test solutions from stock solutions just before use.
4. Immobilize the rpe tissue fragment and seal it in a pre-made perfusion system.
5. Add pre-made pharmacological test agent solution to the donor chamber. Carefully inject prepared buffer into the acceptor chamber.
6. Incubate the perfusion system at 37 °C for 30 min.
7. Quantitatively collect solutions from both chamber compartments.
8. Perform quantitative analysis with HPLC, mass spectrometry and fluorometry.
9. Calculate the permeability coefficient.

9. Essential literature references

Refs. [12,28,37]

References

[1] Clinical Pharmacology, Electronic Drug Reference and Drug Therapy Management Site: http://cp.gsm.com/, 2000.
[2] G. Aguirre, L. Rubin, Diseases of the retinal pigment epithelium in animals, in: K.M. Zinn, M.F. Marmor (Eds.), The Retinal Pigment Epithelium, Harvard Univ. Press, Cambridge, MA, 1979, pp. 334–356.
[3] M. Araie, D.M. Maurice, The loss of fluorescein, fluorescein glucuronide and fluorescein isothiocyanate dextran from the vitreous by the anterior and retinal pathways, Exp. Eye Res. 52 (1991) 27–39.
[4] G.W. Caldwell, S.M. Easlick, J. Gunnet, J.A. Masucci, K. Demarest, In vitro permeability of eight beta-blockers through Caco-2 monolayers utilizing liquid chromatography/electrospray ionization mass spectrometry, J. Mass Spectrom. 33 (1998) 607–614.
[5] R.E. Carr, I.M. Siegel, Clinical evaluation of retinal pigment epithe-

lial disorders, in: K.M. Zinn, M.F. Marmor (Eds.), The Retinal Pigment Epithelium, Harvard Univ. Press, Cambridge, MA, 1979, pp. 381–412.

[6] E.C. Chew, C.T. Liew, S.B. Chew, J.C.K. Lee, H.J. Hou, H.F. Yam, P.C.P. Ho, S.M. Ip, The growth and behavior of pig retinal pigment epithelial cells in culture, In Vivo 7 (1993) 425–430.

[7] J.G. Cunha-Vaz, The blood–ocular barriers, Surv. Ophthalmol. 23 (1979) 279–296.

[8] M.-P. Dehouck, P. Jolliet-Riant, F. Brée, J.-C. Fruchart, R. Cecchelli, J.-P. Tillement, Drug transfer across the blood–brain barrier: correlation between in vitro and in vivo models, J. Neurochem. 58 (1992) 1790–1797.

[9] L.V. Del Priore, B.M. Glaser, H.A. Quigley, M.E. Dorman, W.R. Green, Morphology of pig retinal pigment epithelium maintained in organ culture, Arch. Ophthalmol. 106 (1988) 1286–1290.

[10] S. Duport, F. Robert, D. Muller, G. Grau, L. Parisi, L. Stoppini, An in vitro blood–brain barrier model: cocultures between endothelial cells and organotypic brain slice cultures, Proc. Natl. Acad. Sci. U. S. A. 95 (1998) 1840–1845.

[11] R.H. Edwards, Drug delivery via the blood–brain barrier, Nat. Neurosci. 4 (2001) 221–222.

[12] C. Framme, K. Kobuch, E. Eckert, J. Monzer, J. Roider, RPE in perfusion tissue culture and its response to laser application. Preliminary report, Ophthalmologica 216 (2002) 320–328.

[13] P.J. Gaillard, A.G. de Boer, Relationship between permeability status of the blood–brain barrier and in vitro permeability coefficient of a drug, Eur. J. Pharm. Sci. 12 (2000) 95–102.

[14] F.G. Ghazanfari, R.R. Stewart, Characteristics of endothelial cells derived from the blood–brain barrier and of astrocytes in culture, Brain Res. 890 (2001) 49–65.

[15] C. Gindorf, A. Steimer, C.M. Lehr, U. Bock, S. Schmitz, E. Haltner, Marker transport across biological barriers in vitro: comparison of cell culture models for the gastrointestinal barrier, the blood–brain barrier and the alveolar epithelium of the lung, Altex 18 (2001) 155–164.

[16] E. Haltner, S. Schmitz, C. Gindorf, J. Ruoff, In vitro permeability studies as a substitute for in vivo studies—which requirements have to be met? Altex 18 (2001) 81–87.

[17] Y.-H. Han, D.H. Sweet, D.-N. Hu, J.B. Pritchard, Characterization of a novel cationic drug transporter in human retinal pigment epithelial cells, J. Pharmacol. Exp. Ther. 296 (2001) 450–457.

[18] C.A. Heth, M.A. Yankauckas, M. Adamian, R.B. Edwards, Characterization of retinal pigment epithelial cells cultured on microporous filters, Curr. Eye Res. 6 (1987) 1007–1019.

[19] T.-C. Ho, L.V. Del Priore, H.J. Kaplan, Tissue culture of retinal pigment epithelium following isolation with a gelatin matrix technique, Exp. Eye Res. 64 (1997) 133–139.

[20] A. Hoff, H. Hämmerle, B. Schlosshauer, Organotypic culture system of chicken retina, Brain Res. Protoc. 4 (1999) 237–248.

[21] B.A. Hughes, R.P. Gallemore, S.S. Miller, Transport mechanisms in the retinal pigment epithelium, in: M.F. Marmor, T.J. Wolfensberger (Eds.), The Retinal Pigment Epithelium, Oxford Univ. Press, New York, 1998, pp. 103–134.

[22] C. Kaven, C.W. Spraul, N. Zavazava, G.K. Lang, G.E. Lang, Thalidomide and prednisolone inhibit growth factor-induced human retinal pigment epithelium cell proliferation in vitro, Ophthalmologica 215 (4) (2001) 284–289(Jul–Aug.).

[23] S. Koyano, M. Araie, S. Eguchi, Movement of fluorescein and its glucuronide across retinal pigment epithelium-choroid, Invest. Ophthalmol. Visual Sci. 34 (1993) 531–538.

[24] S. Koyano, M. Araie, S. Eguchi, Movement of fluorescein and its glucuronide across retinal pigment epithelium-choroid, Invest. Ophthalmol. Visual Sci. 34 (1993) 531–538.

[25] T. Kuwabara, Species differences in the retinal pigment epithelium,

in: K.M. Zinn, M.F. Marmor (Eds.), The Retinal Pigment Epithelium, Harvard Univ. Press, Cambridge, 1979, pp. 58–82.

[26] S.P.Letrent,J.W.Polli,J.E.Humphreys,G.M.Pollack,K.R.Brouwer,Brouwer, Brouwer, K.L.R. Brouwer, P-glycoprotein-mediated transport of morphine in brain capillary endothelial cells, Biochem. Pharmacol. 58 (1999) 951–957.

[27] L. Lu, L. Kam, M. Hasenbein, K. Nyalakonda, R. Bizios, A. Young, J.F. Young, A.G. Mikos, Retinal pigment epithelial cell function on substrates with chemically micropatterned surfaces, Biomaterials 20 (1999) 2351–2361.

[28] M.F. Marmor, Comparative and evolutionary aspects of the retinal pigment epithelium, in: M.F. Marmor, T.J. Wolfensberger (Eds.), The Retinal Pigment Epithelium, Oxford Univ. Press, New York, 1998, pp. 23–37.

[29] K. Mertsch, R.F. Haseloff, M.L. Schroeter, I.E. Blasig, In vitro models of the blood–brain barrier for the investigation of cerebroprotective agents, Lebenswissenschaften 3 (1999) 99–124.

[30] J.J. Miguel-Hidalgo, X.A. Alvarez, R. Cacabelos, G. Quack, Neuroprotection by memantine against neurodegeneration induced by beta-amyloid(1–40), Brain Res. 958 (2002) 210–221.

[31] D.S. Miller, S.N. Nobmann, H. Gutmann, M. Toeroek, J. Drewe, G. Fricker, Xenobiotic transport across isolated brain microvessels studied by confocal microscopy, Mol. Pharmacol. 58 (2000) 1357–1367.

[32] B. Moldow, B. Sander, M. Larsen, H. Lund-Andersen, Effects of acetazolamide on passive and active transport of fluorescein across the normal BRB, Invest. Ophthalmol. Visual Sci. 40 (1999) 1770–1775.

[33] M. Palmero, J.L. Bellot, P. Castillo, C. Garcia-Cabanes, J. Miquel, A. Orts, An in vitro model of ischemic-like stress in retinal pigmented epithelium cells: protective effects of antioxidants, Mech. Ageing Dev. 114 (3) (2000) 185–190 (Apr. 14).

[34] Y. Persidsky, Model systems for studies of leukocyte migration across the blood–brain barrier, J. Neurovirology 5 (1999) 579–590.

[35] B. Reisberg, R. Doody, A. Stoffler, F. Schmitt, S. Ferris, H.J. Mobius, Memantine in moderate-to-severe Alzheimer's disease, N. Engl. J. Med. 348 (2003) 1141–1333.

[36] L.L. Rubin, J.M. Staddon, The cell biology of the blood–brain-barrier, Annu. Rev. Neurosci. 22 (1999) 11–28.

[37] B. Schlosshauer, H. Steuer, Comparative anatomy, physiology and in vitro models of the blood–brain and blood–retina barrier, Curr. Med. Chem. 2 (2002) 175–186.

[38] B. Streel, C. Zimmer, R. Sibenaler, A. Ceccato, Simultaneous determination of nifedipine and dehydronifedipine in human plasma by liquid chromatography-tandem mass spectrometry, J. Chromatogr., B., Biomed. Sci. Appl. 720 (1998) 119–128.

[39] T.H. Tezel, L.V. Del Priore, Density-dependent growth regulation of pig retinal pigment epithelial cells in vitro, Graefe's Arch. Clin. Exp. Ophthalmol. 234 (1996) S89–S95.

[40] C.H. To, S.A. Hodson, The glucose transport in retinal pigment epithelium is via passive facilitated diffusion, Comp. Biochem. Physiol. 121 (1998) 441–444.

[41] S.A. Vinores, Assessment of blood–retinal barrier integrity, Histol. Histopathol. 10 (1995) 141–154.

[42] A.N. Wadworth, D. Murdoch, R.N. Brogden, Atenolol. A reappraisal of its pharmacological properties and therapeutic use in cardiovascular disorders, Drugs 42 (1991) 468–510.

[43] I. Walker, M.D. Coleman, The blood–brain barrier: in vitro methods and toxicological applications, Toxicol. In Vitro 9 (1995) 191–204.

[44] H. Wolburg, W. Risau, Formation of the blood–brain barrier, in: H. Keltenmann, B.R. Ransom (Eds.), Neuroglia, Oxford Univ. Press, New York, 1995, pp. 763–776.

[45] K.M. Zinn, J.V. Benjamin-Henkind, Anatomy of the human retinal pigment epithelium, in: K.M. Zinn, M.F. Marmor (Eds.), The Retinal Pigment Epithelium, Harvard Univ. Press, Cambridge, MA, 1979, pp. 3–31.